

Heterodyne measurement of resonant elastic scattering from epitaxial quantum dots

Michael Metcalfe, Glenn S. Solomon, and John Lawall

Citation: *Appl. Phys. Lett.* **102**, 231114 (2013); doi: 10.1063/1.4809594

View online: <http://dx.doi.org/10.1063/1.4809594>

View Table of Contents: <http://apl.aip.org/resource/1/APPLAB/v102/i23>

Published by the [American Institute of Physics](http://www.aip.org).

Additional information on *Appl. Phys. Lett.*

Journal Homepage: <http://apl.aip.org/>

Journal Information: http://apl.aip.org/about/about_the_journal

Top downloads: http://apl.aip.org/features/most_downloaded

Information for Authors: <http://apl.aip.org/authors>

ADVERTISEMENT

a sampling
of our
products



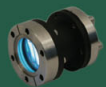
for surface
and materials
science

www.
rbdinstruments
.com

celebrating over
20 years
of innovation



deposition
tools



desorption
systems



sputter
ion sources



viewports



usb
picoammeters

Heterodyne measurement of resonant elastic scattering from epitaxial quantum dots

Michael Metcalfe,¹ Glenn S. Solomon,^{2,1} and John Lawall²

¹The Joint Quantum Institute, 2207 Computer and Space Sciences Bldg., University of Maryland, College Park, Maryland 20742, USA

²National Institute of Standards and Technology, 100 Bureau Dr., Gaithersburg, Maryland 20899, USA

(Received 21 December 2012; accepted 10 May 2013; published online 11 June 2013)

Resonant elastic scattering from InAs quantum dots (QDs) is studied by heterodyne spectroscopy. We show theoretically that heterodyne spectroscopy of a two-level quantum emitter is not sensitive to the inelastic fluorescence component. In practice, we easily measure the elastic emission even when the fluorescence is dominated by inelastic scattering. We are able to distinguish the resonant elastic fluorescence from a large background of scattered pump light by modulating the QD transition frequency with a surface acoustic wave. The signal linewidth is 250 Hz, limited by vibration-induced phase noise in the optical fibers used for resonant optical drive and fluorescence collection. © 2013 AIP Publishing LLC. [<http://dx.doi.org/10.1063/1.4809594>]

Self-assembled InAs quantum dots (QD), nanometer-sized isolated islands of InAs epitaxially embedded in a GaAs matrix, can be described as optically active solid-state “atoms” with discrete energy levels. Using recently developed resonant-spectroscopy techniques, such as differential transmission,¹ cross polarization,² and waveguide coupling,³ two levels (e.g., crystal ground state and the exciton excited state) of the QDs can be optically addressed, thus, revealing quantum-optical properties such as Rabi oscillations,^{4,5} AC Stark effect,⁶ Autler-Townes splitting,^{6–8} and the Mollow Triplet.^{2,9} An enabling feature of these techniques is the ability to reject a large background of scattered resonant pump light while still collecting the QD emission with high efficiency.

When an ideal two-level system (TLS) is driven on resonance, the emission spectrum consists of an elastic component (Rayleigh scattering), which has the spectral properties of the resonant pump laser, and an inelastic component (Mollow spectrum). For large optical drive power P_{opt} , the latter consists of a central peak and two symmetric sidebands separated from the central peak by the Rabi frequency,¹⁰ $\Omega_R = C\sqrt{P_{opt}}$, where C is a constant. The linewidths of these inelastic features are determined by the radiative linewidth of the QD transition, Γ . Previously, the QD Mollow spectrum was resolved with a scanning Fabry-Perot (F-P) interferometer.^{6,9,11–13} However, at large pump powers, the inelastic Mollow spectrum dominates and obscures the weak elastic Rayleigh scattering. In this work, we demonstrate that heterodyne spectroscopy can resolve the Rayleigh signal for even the largest resonant pump powers, with a resolution limited only by vibration-induced phase noise in our optical fibers. We verify that the Rayleigh emission has the spectral properties of the resonant pumping laser and we characterize the magnitude of the elastic signal versus resonant pump power. Furthermore, by strain modulating the QD resonance frequency with a surface acoustic wave (SAW), we are able to distinguish the resonant QD signal from the strongly scattered resonant pump light, thus, eliminating the need for complicated resonant spectroscopy setups.

Our experimental setup is shown in Fig. 1. InAs quantum dots are embedded in a planar AlAs/GaAs distributed Bragg reflector (DBR) cavity. Interdigitated transducers (IDTs) fabricated on the chip surface may be used to excite surface acoustic waves at a frequency of ν_{SAW} ($\nu_{SAW} = 92$ MHz in this work). The SAW applies periodic strain to the QDs, thus, inducing sidebands in their emission spectra.¹⁴ The sample is maintained at a temperature of approximately 3 K in vacuum in a closed-cycle cryostat. The QDs can be resonantly driven with a narrowband CW laser either through the side of the chip, thus, coupling into the DBR planar waveguide or perpendicular to the surface of the chip. The resulting QD emission is collected perpendicular to the sample surface in both cases. As observed previously,^{6,15} a “repumping” laser is required to avoid the QD becoming trapped via an alternative decay path into a state that does not couple to the monochromatic excitation. For the repumper, we use light with a wavelength of 790 nm, with a power level far too low to produce an appreciable photoluminescence signal. Optical excitation and signal collection are done by means of single-mode fibers. We estimate our collection efficiency to be less than 1%. Once outside the cryostat, we measure the QD emission using heterodyne spectroscopy by beating the QD signal, E_{QD} , against a local oscillator, E_{LO} , derived by frequency-shifting light from the excitation laser with an acousto-optic modulator (AOM) driven at frequency ν_{AOM} . The heterodyne signal is then collected with an avalanche photodetector (bandwidth 1 GHz) whose output is measured on a spectrum analyzer.

We now discuss the shot-noise limited sensitivity of heterodyne spectroscopy applied to fluorescence from a single quantum TLS. In the case of an ideal TLS with an electric-dipole coupling to the radiation field, driven on resonance with monochromatic light of power P_{opt} , the spectral density (all spectral densities are taken single-sided in this work) of the total power scattered is given by¹⁰

$$S_{P_{TLS}}^{tot}(\omega) = \frac{\hbar\omega_0}{2}\Gamma g(\Omega_R, \omega), \quad (1)$$

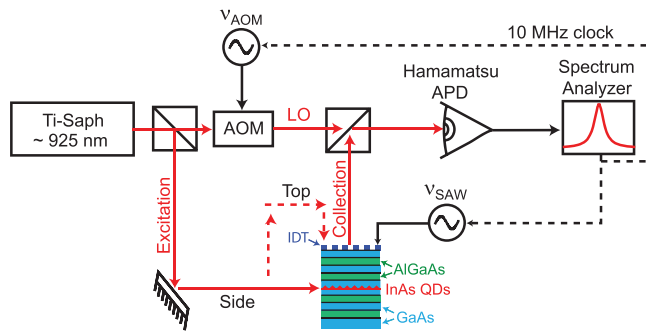


FIG. 1. Schematic of heterodyne measurement setup. The quantum dots can be resonantly excited through the side of the chip into the planar waveguide. This minimizes the amount of scattered resonant pump light entering the collection optics. By modulating the QD resonance frequency at rf frequencies using a SAW, however, we can use the heterodyne technique to extract the resonant QD signal even when exciting the QD and extracting the fluorescence perpendicular to the surface of the chip using the same optics.

where $\Omega_R = C\sqrt{P_{opt}}$ and $\hbar\omega_0$ is the separation in energy between the levels of the TLS. Here, $g(\Omega_R, \omega)$ is the sum of an elastic component

$$g_{el}(\Omega_R, \omega) = \frac{4\pi\Gamma^2\Omega_R^2}{(\Gamma^2 + 2\Omega_R^2)^2} \delta(\omega - \omega_0) \quad (2)$$

and an inelastic component $g_{inel}(\Omega_R, \omega)$, the Mollow spectrum. For low Rabi frequency $\Omega_R \ll \Gamma$, the spectrum is dominated by the elastic scattering. As the resonant excitation power is raised, the inelastic emission becomes more significant, and for $\Omega_R \gg \Gamma$, the spectrum is dominated by the three inelastic peaks (“Mollow triplet”).

Heterodyne spectroscopy allows us to shift the optical spectrum to a frequency where it is accessible by means of rf electronics. We next relate the power spectrum of the heterodyne signal to the power spectrum of the QD emission. To this end, we assume that some fraction of the scattered QD emission is collected and collimated, and beat it with a strong monochromatic optical local oscillator (LO) with frequency ν_{LO} , such that the frequency ν_{LO} is near the characteristic frequency ν_{QD} of the QD emission. We take the electric field of our LO to have the same transverse spatial dependence and polarization as the signal beam (perfect spatial mode overlap). The total electric field $E_{tot} = E_{LO} + E_{QD}$ is incident on a square-law detector, which gives a signal V proportional to the instantaneous optical power, with constant of proportionality K . It is the sum of a DC term $V_{DC} = K(P_{LO} + P_{QD}) \approx KP_{LO}$ and an AC term $V_{AC}(t)$. Taking the autocorrelation of $V_{AC}(t)$ and using the Wiener-Khinchin theorem, one finds that the spectral density of the heterodyne signal power is related to the power spectral density $S_{P_{QD}}(\omega)$ of the QD emission by¹⁶

$$S_{V_{AC}}(\omega) = 2P_{LO}K^2\{S_{P_{QD}}(\omega + \omega_{LO}) + S_{P_{QD}}(\omega_{LO} - \omega)\}, \quad (3)$$

where $\omega_{LO} = 2\pi\nu_{LO}$.

It is desirable to choose a local oscillator frequency that is either larger or smaller than all frequency components in the signal, so that one of the terms in Eq. (3) vanishes. Henceforth, we assume the latter condition, so that $S_{V_{AC}}(\omega) = 2P_{LO}K^2S_{P_{QD}}(\omega + \omega_{LO})$. It is thus apparent that

the result of the heterodyne measurement is to shift the power spectrum by an amount ω_{LO} , from the optical to the rf domain, and scale it by a factor $2P_{LO}K^2$.

The minimum possible measurement noise will be the shot noise associated with the DC term V_{DC} . To determine the shot-noise limit, we take $K = \eta/(\hbar\omega_{LO})$, where η is the detector quantum efficiency. The shot-noise limited S/N ratio¹⁶ for the elastic Rayleigh signal is then found to be

$$\left. \frac{S}{N} \right|_{elastic} = \frac{\eta}{B} \frac{\Gamma^3\Omega_R^2}{(\Gamma^2 + 2\Omega_R^2)^2} \quad (4)$$

in the event that all of the scattered fluorescence is captured. This is maximized for $\Omega_R = \Gamma/\sqrt{2}$, at which point $S/N|_{elastic,max} = \eta\Gamma/(8B)$. It is noteworthy that the S/N ratio is independent of the power of the local oscillator laser. In practice, the LO power should be chosen high enough that its shot noise dominates the detector dark noise, but low enough to avoid detector saturation.

The shot-noise limited S/N ratio for the inelastic signal is found to be

$$\left. \frac{S}{N} \right|_{inelastic} = \frac{\eta}{2} \Gamma g_{inel}(\Omega_R, \omega + \omega_{LO}) \quad (5)$$

independent of bandwidth. Fig. 2 shows the theoretical shot-noise limited S/N ratio from Eqs. (4) and (5) for heterodyne observation of the resonantly driven QD fluorescence, assuming a quantum efficiency $\eta = 1$, radiative linewidth $\Gamma = 10^9 \text{ s}^{-1}$, and a measurement bandwidth of $B = 1 \text{ Hz}$. Rabi frequencies of $\Omega_R = \Gamma/\sqrt{2}$ (maximum elastic S/N), $\Omega_R = 2\Gamma$ (maximum inelastic S/N), and $\Omega_R = 8\Gamma$ (well-resolved Mollow triplet) have been chosen, each with a different heterodyne frequency for clarity. The elastic spectrum has an S/N ratio of up to 1.25×10^8 (81 dB) in a 1-Hz bandwidth. In practice, of course, the value will be substantially lower, primarily because one typically collects only a small fraction of the total emission from a single QD. As seen in Fig. 2, however, the S/N ratio of the inelastic part of the

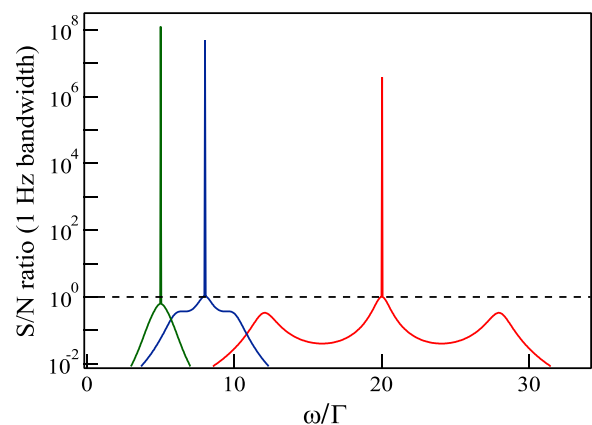


FIG. 2. Shot-noise limited S/N ratio for heterodyne signal from a single quantum emitter with $\Gamma = 10^9 \text{ s}^{-1}$ for the cases (left, green) $\Omega_R = \Gamma/\sqrt{2}$, $\omega_{LO} = 5\Gamma$, (middle, blue) $\Omega_R = 2\Gamma$, $\omega_{LO} = 8\Gamma$, (right, red) $\Omega_R = 8\Gamma$, $\omega_{LO} = 20\Gamma$; different heterodyne frequencies ω_{LO} are taken for clarity. In all cases, it is assumed that all of the scattered light is captured and the detector has unit quantum efficiency. The inelastic part of the spectrum falls below the noise floor.

Mollow triplet as observed in heterodyne spectroscopy always falls below unity. Thus, the inelastic fluorescence from a single QD will never be observable with heterodyne spectroscopy, regardless of the amount of integration time. The same conclusion can be shown to apply to the case of QD photoluminescence with a Lorentzian spectral density.¹¹

A typical measured heterodyne signal is shown in Fig. 3. The QD is modulated with a SAW at $\nu_{\text{SAW}} = 92$ MHz, and heterodyne signals from the sideband fluorescence are observed at $\nu_{\text{SAW}} \pm \nu_{\text{AOM}}$, despite the presence of a background of scattered resonant pump light that is orders of magnitude larger than the signal of interest. The red curve shows a high-resolution heterodyne spectrum of one sideband, offset by $\nu_{\text{offset}} \equiv \nu_{\text{SAW}} + \nu_{\text{AOM}}$ (172 MHz). The blue curve shows the resonant elastic signal when the repumping laser is blocked. No QD signal is observed, confirming that the heterodyne signal we observe comes from QD emission and is not an electronic artifact or scattered pump light.

Since the local oscillator is derived from the same laser as the one driving the resonant QD emission, the linewidth of the heterodyne signal should be unaffected by the optical frequency fluctuations contributing to the laser linewidth (≈ 500 kHz). The data in Fig. 3 were taken with a resolution bandwidth of 100 Hz, and the FWHM of the heterodyne signal is measured to be 250 ± 20 Hz. To further understand the observed linewidth, we performed two auxiliary experiments. In a first case, we detuned the pump from the QD to eliminate QD emission and used nonresonant light scattered off the vacuum/GaAs interface on our sample as the “signal.” We observed a heterodyne signal with the same FWHM, shifted of course by ν_{SAW} (92 MHz) from that shown in Fig. 3. A second comparison was made with a signal produced by mixing the pump laser directly with the LO, bypassing the cryostat and the collection/excitation fibers. In this case, the observed signal was much narrower, limited by the resolution bandwidth of our spectrum analyzer (20 Hz). We infer that the dominant source of broadening in our observed signal is likely to be phase noise contributed by the optical fiber used for excitation and emission extraction.

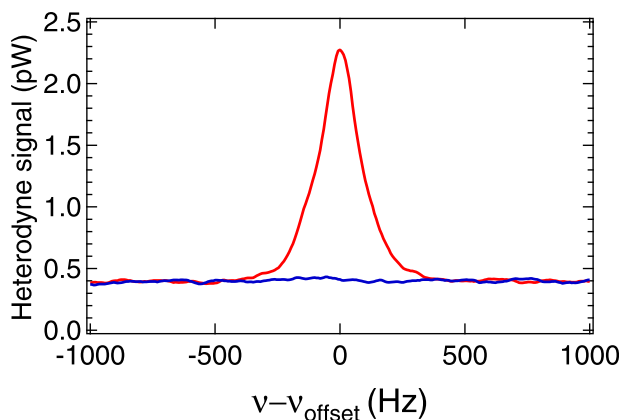


FIG. 3. Typical heterodyne signal measured on spectrum analyzer. The local oscillator is offset from the excitation laser by 80 MHz, the QD energy levels are modulated using a SAW at 92 MHz, and the sidebands generate beat notes at 12 MHz and 172 MHz. Red curve: Signal at 172 MHz, offset by $\nu_{\text{offset}} \equiv \nu_{\text{SAW}} + \nu_{\text{AOM}}$. The spectrum analyzer resolution bandwidth is set to 100 Hz. Blue curve: Background signal when the QD emission is “switched off” by extinguishing the repumper.

Thus, as expected, the elastic spectrum is determined by the properties of the resonant pump laser and not by intrinsic properties of the QD.

Finally, we use our heterodyne technique to track the elastically scattered QD fluorescence for all resonant pump powers and compare it to that predicted by Eq. (2). We begin by calibrating the Rabi frequency, Ω_R , vs resonant pump power, P_{opt} , by measuring the complete fluorescence spectrum with a scanning FP cavity¹¹ while resonantly exciting the QD from the side through the planar waveguide. The QD linewidth Γ and Rabi frequency Ω_R are extracted by fitting fluorescence spectra such as those shown in Fig. 4(a) to an analytical convolution of the power spectrum (1) with the Lorentzian response of our FP cavity (FWHM 210 MHz). Prior to performing these fits, the background, measured by extinguishing the repumping laser, has been subtracted, so that any contribution from residual scattered pump light has been eliminated. In this manner, we determine the Rabi frequency as a function of optical power for a range of powers spanning more than three orders of magnitude. The inset to Fig. 4(a) shows the data, along with a fit to $\Omega_R = C\sqrt{P_{\text{opt}}}$ yielding $C = 0.03 \pm 0.002$ GHz/ $\mu\text{W}^{0.5}$. From the fits, we also infer the QD linewidth $\Gamma/(2\pi) = 508 \pm 20$ MHz. The uncertainties refer to the standard deviation of results from three complete scans of resonant drive power. It is notable that there is a distinct kink in the data for $\Omega_R \approx \Gamma$ ($P_{\text{opt}} \approx 400$ μW), in the intermediate region between

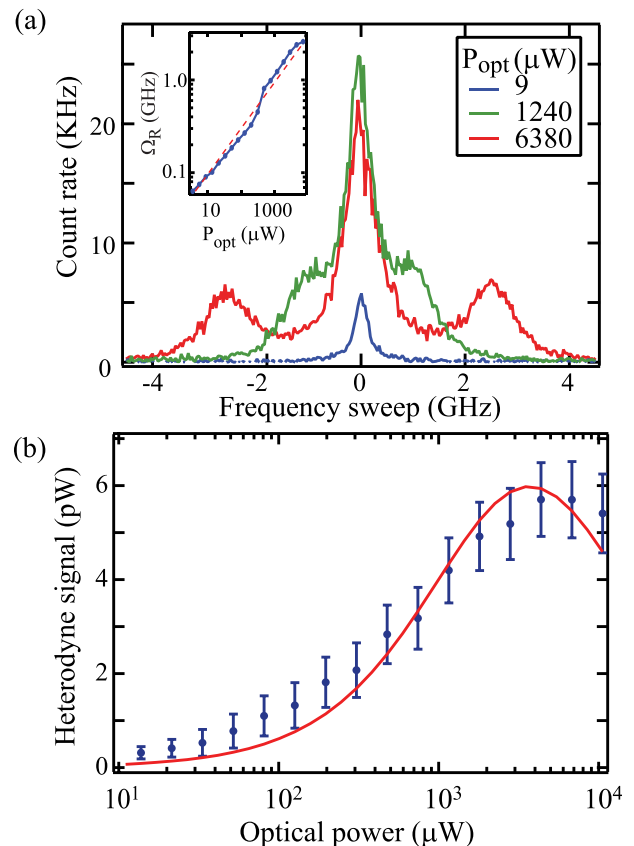


FIG. 4. (a) Mollow triplet measured using a scanning FP interferometer for three different resonant drive powers. Elastic emission is visible at low pump powers (blue curve), but not distinguishable from inelastic emission at high pump powers (green and red curves). Inset: Result of fitting 18 such curves to the Mollow expression to extract Ω_R . (b) Heterodyne signal power versus input optical pump power for the same QD. The red curve is a fit to Eq. (2).

the elastic and inelastic regimes, suggestive of a departure from the exact description of a resonantly driven two-level system.

We now proceed to the heterodyne measurement, which filters out the inelastic Mollow emission that dominates the FP data at high pump powers. As in Fig. 3, the QD is modulated at $\nu_{\text{SAW}} = 92$ MHz and we study the heterodyne signal at $\nu_{\text{SAW}} + \nu_{\text{AOM}} = 172$ MHz. Fig. 4(b) shows (blue circles) the heterodyne signal as a function of the optical drive power. The red line is a fit to Eq. (2), taking $\Omega_R = C\sqrt{P_{\text{opt}}}$; the extracted value of $C = 0.006 \pm 0.0006$ GHz/ $\mu\text{W}^{0.5}$ is found to differ rather substantially from that obtained with the Mollow data. Once again the stated uncertainty corresponds to the standard deviation of fits from three different scans. We have observed similar behavior, with the expected clear reduction of the signal at high pump powers, on other samples with SAWs at 90 MHz, 500 MHz, and 1 GHz. The discrepancy between the Rabi frequency inferred from the inelastic and elastic data suggests a departure from the ideal two-level-system behavior described by Eq. (1). A QD has alternative optical transitions in the vicinity of the one studied, and it is embedded in a GaAs matrix resulting in possible couplings to nearby defects and carriers. As mentioned previously, the kink observed in the inset of Fig. 4(a) is suggestive of non-ideal two-level behavior. Furthermore, the fact that a repumper is required to avoid population trapping and the corresponding fluorescence quenching are additional evidence of nearby states not accounted for in the simple TLS theory. In addition, phonons from the SAW may be playing a role (the SAW is not applied while measuring the inelastic spectra). These matters are under investigation.

In conclusion, we have described and implemented a heterodyne technique to perform resonant spectroscopy of a single self assembled InAs/GaAs QD. The method is shown theoretically to be sensitive only to the elastic component of the fluorescence, and indeed we find experimentally that the elastic signal can be resolved for all resonant pump powers, even deep in the inelastic regime. The linewidth of the heterodyne signal is below our measurement resolution of 250 Hz, in agreement with the expected nature of Rayleigh elastic scattering. Furthermore, by fast modulation of the QD

resonance frequency, the heterodyne technique enables the QD signal to be measured even in the presence of strongly scattered resonant pump light. Future perspectives for this work include full phase control of the heterodyne signal, enabling coherent detection of perturbations of the QD.

The authors would like to thank E. B. Flagg, G. Bryant, A. Muller, and J. Taylor for fruitful discussions throughout this work. During production of this paper, we became aware of new work¹⁷ of a similar nature. We acknowledge support by NSF through the Physics Frontier Center at JQI. Research performed in part at the NIST Center for Nanoscale Science and Technology.

- ¹K. Karrai and R. J. Warburton, *Superlattices Microstruct.* **33**, 311 (2003).
- ²A. N. Vamivakas, Y. Zhaol, C. Lu, and M. Atatüre, *Nat. Phys.* **5**, 198 (2009).
- ³A. Muller, E. B. Flagg, P. Bianucci, X. Y. Wang, D. G. Deppe, W. Ma, J. Zhang, G. J. Salamo, M. Xiao, and C. K. Shih, *Phys. Rev. Lett.* **99**, 187402 (2007).
- ⁴T. H. Stievater, X. Li, D. G. Steel, D. Gammon, D. S. Katzer, D. Park, C. Piermarocchi, and L. J. Sham, *Phys. Rev. Lett.* **87**, 133603 (2001).
- ⁵H. Kamada, H. Gotoh, J. Temmyo, T. Takagahara, and H. Ando, *Phys. Rev. Lett.* **87**, 246401 (2001).
- ⁶A. Muller, W. Fang, J. Lawall, and G. S. Solomon, *Phys. Rev. Lett.* **101**, 027401 (2008).
- ⁷X. Xu, B. Sun, P. R. Berman, D. G. Steel, A. S. Bracker, D. Gammon, and L. J. Sham, *Science* **317**, 929 (2007).
- ⁸G. Jundt, L. Robledo, A. Högele, S. Fält, and A. Imamoglu, *Phys. Rev. Lett.* **100**, 177401 (2008).
- ⁹E. B. Flagg, A. Muller, J. W. Robertson, S. Founta, D. G. Deppe, M. Xiao, W. Ma, G. J. Salamo, and C. K. Shih, *Nat. Phys.* **5**, 203 (2009).
- ¹⁰M. O. Scully and M. S. Zubairy, *Quantum Optics* (Cambridge University Press, 1997).
- ¹¹M. Metcalfe, A. Muller, G. S. Solomon, and J. Lawall, *J. Opt. Soc. Am. B* **26**, 2308 (2009).
- ¹²C. Matthiesen, A. N. Vamivakas, and M. Atatüre, *Phys. Rev. Lett.* **108**, 093602 (2012).
- ¹³S. M. Ulrich, S. Ates, S. Reitzenstein, A. Löffler, A. Forchel, and P. Michler, *Phys. Rev. Lett.* **106**, 247402 (2011).
- ¹⁴M. Metcalfe, S. M. Carr, A. Muller, G. S. Solomon, and J. Lawall, *Phys. Rev. Lett.* **105**, 037401 (2010).
- ¹⁵H. S. Nguyen, G. Sallen, C. Voisin, P. Roussignol, C. Diederichs, and G. Cassabois, *Phys. Rev. Lett.* **108**, 57401 (2012).
- ¹⁶See supplementary material at <http://dx.doi.org/10.1063/1.4809594> for details.
- ¹⁷C. Matthiesen, M. Geller, C. H. Schulte, C. L. Gall, J. Hansom, Z. Li, M. Hugues, E. Clarke, and M. Atatüre, *Nat. Commun.* **4**, 1600 (2013).